Chapter 1

fNIRS-Based Clinical Assessment of ADHD Children

Yukifumi Monden, Masako Nagashima,
Haruka Dan, Takahiro Ikeda, Yasushi Kyutoku,
Takanori Yamagata and Ippeita Dan

Additional information is available at the end of the chapter

http://dx.doi.org/10.5772/intechopen.71835

Abstract

While a growing body of neurocognitive research has explored the neural substrates associated with attention deficit hyperactive disorder (ADHD), an objective biomarker for diagnosis has not been established. The advent of functional near-infrared spectroscopy (fNIRS), which is a noninvasive and unrestrictive method of functional neuroimaging, raised the possibility of introducing functional neuroimaging diagnosis for young ADHD children. In search of a stable and clinically applicable biological marker, here in this chapter, we first discuss a plausible solution to enable the objective monitoring of the acute effects of ADHD medications at the group level. Subsequently, we discuss our successful visualization of differential neural substrates between ADHD and healthy control children for inhibitory control at the individual level, which reached an optimized classification parameter with a value of 85% and a sensitivity of 90%. These findings led us to postulate that fNIRS-based examination would allow the identification of an objective neuro-functional biomarker to diagnose and determine the appropriate treatment for ADHD children. We believe that such a novel technical application would evoke wide interest from neuroimaging researchers.

Keywords: developmental syndromes, optical topography, response inhibition, autism, discrimination analysis

1. Introduction

Noninvasive functional neuroimaging has been introduced as a promising approach, in combination with psychological tests, to clinical diagnosis. Functional near-infrared spectroscopy (fNIRS) is an increasingly popular neuroimaging technique which noninvasively monitors human brain activation patterns, utilizing the tight coupling between neural activity and

regional cerebral hemodynamic responses, which has a high affinity with the study of developing brains (reviewed in, for example, [1–5]).

fNIRS has distinct advantages in its compactness, tolerance to body motion, affordable price, and accessibility [2, 6–11]. These advantages allow fNIRS to be contrasted with conventional imaging modalities such as functional magnetic resonance imaging (fMRI), single photon emission computed tomography (SPECT), positron emission tomography (PET), and magnetoencephalography (MEG), which are susceptible to motion artifacts and are performed using large apparatuses. Conversely, we expect fNIRS to occupy a unique position among neuroimaging methods: to provide complementary usage in clinical settings, such as bedside situations, for the purposes of diagnosis and treatment [8].

Indeed, fNIRS has been applied in various clinical studies including assessment of the outcome of neurologic rehabilitation for pathological gait [12], monitoring of ischemia [13], monitoring of language dominance before neurosurgery [14], identification of epileptic focus [15, 16], making a diagnosis of various neurological and psychiatric diseases [8, 17], and so on. Furthermore, in Japan, the first clinical applications of fNIRS in neurosurgery, assessment of hemispheric dominance for language function [14], detection of epileptic focus [15], and aid for differential diagnosis of depressive symptoms, have been included under National Health Insurance coverage. There are, indeed, great expectations for the application of fNIRS in various clinical situations, such as the exploration of objective diagnoses for developmental disorders and dementia as well as treatment assessment of medication intervention and rehabilitation. Among these, one of the most promising clinical applications of fNIRS, for which its convenience and robustness would be highly appreciated, is the functional monitoring of ADHD children, who have difficulty performing active cognitive tasks in the enclosed environments of other imaging modalities such as fMRI, PECT, PET, and MEG. A growing body of fNIRS studies has started to investigate the cortical hemodynamics of ADHD patients [18–23].

Attention deficit hyperactivity disorder (ADHD) is one of the most common psychiatric disorders in children. It affects between 3 and 7% of early elementary school children with typical behavioral symptoms of inattention, impulsivity, and hyperactivity [24, 25]. While ADHD is often diagnosed between the ages of 4 and 6 [26], ADHD symptoms are not specific to childhood, and 75–85% of patients are estimated to continue experiencing symptoms through adolescence and adulthood [27]. Consequently, 4–5% of adults have recently been reported to have ADHD [28]. Therefore, early identification and appropriate treatment are considered important in order to increase the quality of life of ADHD patients [29]. Today, the diagnosis of ADHD depends mainly on interview-based evaluation of the degrees of the phenotypes according to diagnostic criteria listed in the DSM-5 as observed by a patient's parents or teachers (http://www.dsm5.org). However, interview-based assessments often entail subjective evaluations by parents and teachers, which present the risk of under or overestimations of ADHD symptoms [30, 31].

ADHD clinical guidelines provide recommended medication treatment, behavioral therapy, and community therapy for ADHD children [32–34]. Furthermore, an American Academy

of Pediatrics (AAP) and MTA study revealed that medication treatment was superior to behavioral therapy for school-aged children over 6 years old [35]. According to copious evidence accumulated over several decades, one of the most commonly recommended treatments has been the administration of psychostimulants and non-psychostimulants, such as methylphenidate (MPH) and atomoxetine (ATX) to improve ADHD symptoms [36]. An objective biomarker of the pharmacological effects is urgently required because current treatment evaluation of ADHD depends on evaluation of the degrees of the symptoms listed in the diagnostic criteria. Interview-based measurements need to be rated by parents or teachers of the children, and thus often tend to entail subjective evaluation. Because of the technical limitations of relying on interview-based clinical observation of ADHD patients, the identification of a biological marker is needed to help facilitate objective assessments of pharmacological responses [37–39].

This led us to postulate that fNIRS would be effective in monitoring the effects of the ADHD medications MPH and ATX, especially in younger children who are difficult to assess using other neuroimaging modalities. The lack of evidence associating a neuropharmacological mechanism to therapeutic improvement is tantamount to a missed opportunity for appreciating how MPH and ATX work in the central nervous system, and such understanding is a vital step toward developing an objective, evidence-based neuropharmacological treatment for ADHD children. Thus, we performed an fNIRS study in order to assess acute neuropharmacological effects of MPH and ATX on the inhibitory functions of ADHD children.

We selected a go/no-go task as the experimental task. Go/no-go task has emerged as a principal paradigm for involving the multidimensional construct of response inhibition that refers to the ability to suddenly and completely stop a planned course of action. It is an essential executive function required in daily life, and impaired response inhibition is a strong candidate for a biomarker for ADHD [40] Former fMRI studies successfully visualized decreased hemodynamic responses with ADHD using motor response inhibition tasks including go/no-go, stop signal, and Stroop tasks [41–45]. Among these tasks, go/no-go task performance matures at approximately 12 years [46], followed by stop signal task at 13–17 years, and lastly, Stroop task at around 17–19 years of age [47, 48]. Therefore, a go/no-go task would be the primary choice for a study of school-aged children. fNIRS studies that presented right VLPFC activation during go/no-go tasks have been replicated [9]. Furthermore, structural neuroimaging studies of ADHD have fairly consistently indicated gray matter density reductions in the striatum and right IFG [49].

Therefore, in two consecutive studies making the most of fNIRS's merits, we have explored the neural substrate of inhibitory controls in school-aged ADHD children for the detection of a clinically-oriented biomarker for ADHD diagnosis and evaluation for ADHD medications. In Study 1, we explored differential neural substrates for ADHD and healthy control children during go/no-go task in group analyses using fNIRS measurement. In Study 2, we explored a method of individual differentiation between ADHD and healthy control children using multichannel fNIRS, emphasizing how the spatial distribution and amplitude of hemodynamic response associated with go/no-go task execution can be utilized.

2. Study1: differential neural substrates for ADHD and healthy control children during go/no-go task in group analyses, using fNIRS measurement

Our initial effort [50] examined whether fNIRS-based monitoring for neuropharmacological effects could be visualized in actual clinical situations. To do so, we demonstrated that fNIRS could detect the cortical hemodynamic responses of ADHD children (7–14 years old) performing a go/no-go task before and 1.5 h after MPH administration, allowing the observation of the acute effect of MPH as a significant increase of hemodynamic (oxy-Hb) response in the right prefrontal cortex. As the monitoring takes about 6 minutes, we further demonstrated that the entire protocol can be implemented within a single-day hospital visit.

However, since that study was optimized for assessing the feasibility of fNIRS monitoring as an actual clinical tool that allows the pre- and post-medication comparison to be performed in a single-day hospital visit, a neuro-pharmacological assessment of the effects of ADHD medications has yet to be performed. Experimental designs should be optimized in a neuropharmacological assessment, including a randomized, double-blind design with comparison to healthy control subjects.

Thus, for the present study, to explore the neuropharmacological assessment of ADHD medications, we enrolled ADHD children and age- and sex-matched healthy control subjects, and examined the neuropharmacological effects of ADHD medications on inhibition control, utilizing a within-subject, double-blind, placebo-controlled design. Additionally, we desire to validate the feasibility of introducing fNIRS-based diagnosis of the effects of ADHD medications, MPH and ATX, for use with ADHD children as young as 6 years old, the earliest age at which the FDA recommends starting MPH and ATX administration. **Figure 1** describes the experimental protocol. We examined the effects of MPH (OROS-methylphenidate commercially available as Concerta) and ATX (Strattera, Eli Lilly and Co., Indianapolis, IN, USA) in a randomized, double-blind, placebo-controlled, crossover study during a go/no-go task. All ADHD patients were pre-medicated with MPH (n = 16) or ATX (n = 16) as part of their regular medication regimen. We performed fNIRS measurements of ADHD subjects twice (the times of day for both measurements were scheduled to be as close as possible), at least 2 days apart, but within 30 days. Control subjects underwent a single, non-medicated session. On each examination procedure day, ADHD subjects underwent two sessions, one before drug (MPH/ATX or placebo) administration, and the other 1.5 h after drug administration. Before each pre-administration session, a washout period of 2–3 days was undertaken by all ADHD subjects. Each session involved 6 each of go (baseline) and go/no-go (target) blocks, which were alternated. Each block lasted 24 s and was preceded by trial instructions displayed on a PC monitor for 3 s, giving an overall block-set time of 54 s and a total session time of about 5.5–6.0 min. In the go blocks, we presented subjects with random sequences of two animal pictures and asked them to press a button for both pictures as quickly as possible. In the go/no-go blocks, we presented subjects with a no-go picture 50% of the time, thus requiring subjects to respond to half the trials (go trials) and inhibit their response to the other half (no-go trials). After ADHD subjects performed the first session, either MPH/ATX or a placebo was administered orally. We generated stimuli and collected responses using E-Prime 2.0

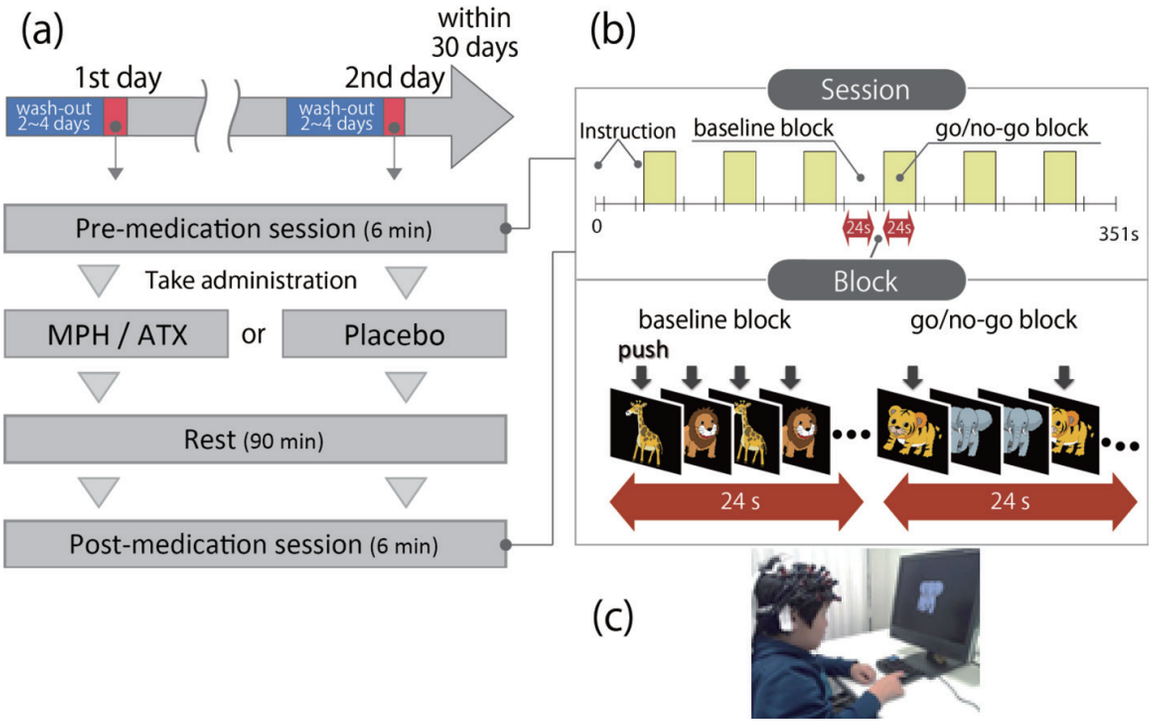

Figure 1. Experimental procedure to detect the differential neural activation pattern for ADHD and healthy control children during go/no-go task in group analyses, using fNIRS measurement. (a) A schematic showing the flow of pre- and post-medication administration sessions for ADHD subjects. (b and c) fNIRS measurements. Brain activity was measured using fNIRS, while ADHD and healthy control subjects performed the go/no-go task.

(Psychology Software Tools). Stimuli were presented to the subject on a 17″ desktop computer screen. The distance between the subject's eyes and the screen was about 50 cm.

We used the multichannel fNIRS system ETG-4000 (Hitachi Medical Corporation, Kashiwa, Japan), which utilizes two wavelengths of near-infrared light (695 and 830 nm). We analyzed the optical data based on the modified Beer-Lambert Law [51] as previously described [52]. This method enabled us to calculate signals reflecting oxygenated hemoglobin (oxy-Hb), deoxygenated hemoglobin (deoxy-Hb), and total hemoglobin (total-Hb) signal changes, obtained in units of millimolar·millimeter (mM·mm) [52]. In order to perform statistical analyses, we treated the oxy-Hb signal as the primary outcome of hemodynamic responses because of its higher sensitivity to changes in cerebral blood flow compared with deoxy-Hb and total-Hb signals [53–55], its higher signal-to-noise ratio [53], and its higher retest reliability [56]. We used two sets of 3x5 multichannel probe holders, which resulted in 22 channels (CH) per set. Each probe holder consisted of eight illuminating and seven detecting probes arranged alternately at an inter-probe distance of 3 cm to cover the lateral prefrontal cortices and inferior parietal lobe, referring to previous studies [9, 57–60]. The midpoint of a pair of illuminating and detecting probes was defined as a channel location. The bilateral probe holders were attached in the following manner: (1) their upper anterior corners, where we connected the right and left probe holders by a belt, were symmetrically placed across the sagittal midline, (2) the lower anterior corners of the probe holder were placed over the supraorbital prominence, and (3) the lower edges of the probe holders were attached at the

upper part of the auricles. Virtual registration was adopted for spatial profiling of fNIRS data [61, 62] to register fNIRS data to MNI standard brain space [63]. This method enables us to place a virtual probe holder on the scalp based on a simulation of the holder's deformation and the registration of probes and channels onto reference brains in an MRI database [64, 65]. Specifically, the positions of channels and reference points, consisting of the Nz (nasion), Cz (midline central), and left and right preauricular points, were measured with a 3D-digitizer in real-world (RW) space. The RW reference points were affine-transformed to the corresponding reference points in each entry in reference to the MRI database in MNI space. We adopted the same transformation parameters to obtain the MNI coordinates for the fNIRS channels and the most likely estimates of the locations of given channels for the group of subjects together with the spatial variability associated with the estimation [66]. Finally, macroanatomical labels were estimated using a Matlab function that reads labeling information coded in macroanatomical brain atlases, LBPA40 [67] and Brodmann's atlas [68].

Individual timeline data for the oxy-Hb and deoxy-Hb signals of each channel were preprocessed with a first-degree polynomial fitting and high-pass filter using cut-off frequencies of 0.01 Hz in order to remove baseline drift, and a 0.8 Hz low-pass filter to remove heartbeat pulsations. In fNIRS measurements, note that the Hb signals analyzed do not directly represent cortical Hb concentration changes, but contain an unknown optical path length that cannot be measured. Direct comparison of Hb signals among different channels and regions should be avoided as optical path length is known to vary among cortical regions [69]. Hence, statistical analyses were performed in a channel-wise manner. We computed channel-wise and subject-wise contrasts by calculating the inter-trial mean of differences in Hb signals between peak (4–24 s after go/no-go block onset) and baseline (14–24 s after go block onset) periods from the preprocessed time series data. We visually inspected the movements of the subjects and removed the blocks with sudden, obvious, discontinuous noise for the six go/no-go blocks. We subjected the resulting contrasts to second-level, random-effects group analyses.

Figure 2 describes the experimental results. The oxy-Hb signals were statistically analyzed in a channel-wise manner. Specifically, for healthy control subjects, who were examined only once, a target (no-go block session) vs. baseline (go block session) contrast was generated (**Figure 2(a)**). For ADHD subjects, we generated the following contrasts: (1) pre-medication contrasts: target vs. baseline contrasts for pre-medication conditions (either placebo or MPH/ATX administration) for the first day exclusively (**Figure 2(b)**), (2) post-medication contrasts: the respective target vs. baseline contrasts for post-placebo and post-MPH/ATX conditions (**Figure 2(c, d)**), and (3) inter-medication contrasts: differences between $\text{MPH/ATX}^{\text{post–pre}}$ and $\text{placebo}^{\text{post–pre}}$ contrasts (**Figure 2(c, d)**). Cortical activation patterns of healthy control subjects (a) and of ADHD subjects (b–d) are shown as t-maps of oxy-Hb signal, with significant t-values (one-sample t-test, $p < 0.05$) being shown according to the color bar.

Firstly, to screen the channels involved in go/no-go tasks in healthy control subjects, paired t-tests (two-tails) were performed on target vs. baseline contrasts. The statistical threshold was set at 0.05 with Bonferroni correction for family-wise errors. We found significant oxy-Hb increase in the right CH 10 (mean 0.075, SD 0.074, $p < 0.05$, Bonferroni-corrected, Cohen's $d = 1.009$; (**Figure 2(a)**). CH 10 was located in the border region between the right MFG and IFG (MNI

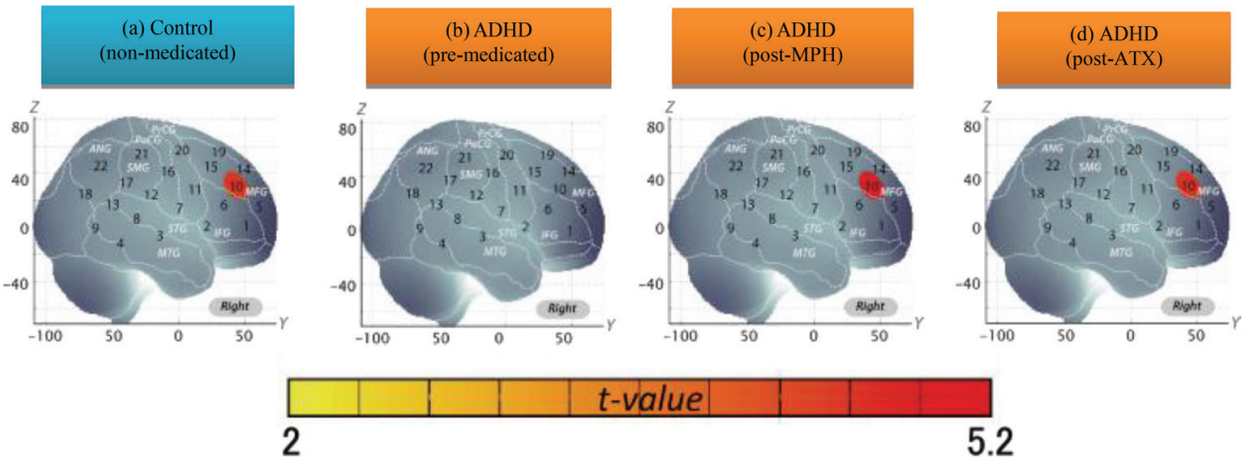

Figure 2. Differences of neuroactivation patterns between ADHD and healthy control during go/no-go task. The channel location of oxy-Hb signals for the right CH 10. (a) Healthy control (b) pre-medicated ADHD (c) post-MPH administration and (d) post-ATX administration.

coordinates *x*, *y*, *z* (SD): 46, 43, 30 (14), MFG 78%, IFG 22% with reference to macroanatomical brain atlases [67, 68]). Therefore, we set the right CH 10 as a region-of-interest (ROI) for the rest of the study. In ADHD conditions, we found that no channels were activated in the pre-medication and post-placebo conditions (**Figure 2(b)**). On the other hand, the right CH 10 exhibited significant oxy-Hb increase in the post-MPH (mean 0.077, SD 0.060, $p < 0.05$, Cohen's $d = 1.283$; (**Figure 2(c)**) and post-ATX (mean 0.074, SD 0.063, $p < 0.05$, Cohen's $d = 1.165$; (**Figure 2(d)**) conditions. Finally, the effects of medications were investigated in the inter-medication contrast: we found the right CH 10 to be significantly different between medication and placebo conditions, MPH (paired *t*-test, $p < 0.05$, Cohen's $d = 0.952$) and ATX (paired *t*-test, $p < 0.05$, Cohen's $d = 0.663$). These results demonstrate that MPH and ATX, but not the placebo, induced an oxy-Hb signal increase during the go/no-go task.

3. Study 1: Discussion

Previous fMRI measurements for healthy control subjects have provided preliminary evidence for the neural correlates of go/no-go tasks [70], including the bilateral IFG, MFG and SFG (superior frontal gyrus), supplementary motor area, anterior cingulate gyrus, inferior parietal and temporal lobes, caudate nucleus, and cerebellum [60]. In addition, recent fMRI [41–45] and fNIRS [71, 72] studies on acute medication effects on ADHD have also shown that bilateral IFG and MFG were robustly normalized after ADHD medications. Taken together, the specificity of the implicated brain regions, such as MFG and IFG, in healthy subjects, as well as functional and structural changes to those regions in ADHD patients, suggests that response inhibition is a good neuro-functional biomarker candidate for ADHD [73].

Our current study found activation in the right MFG and IFG (BA9, 46, 45) during the go/no-go task period in the healthy control subjects, but not in the pre-medicated ADHD subjects. These results suggest that ADHD produces impairment of right prefrontal function

associated with go/no-go task performance. The administration of MPH and ATX led to a degree of right prefrontal activation in ADHD children comparable to that of the healthy control subjects, but the placebo did not. These results suggest that as observed using fNIRS, normalized right IFG/MFG activation associated with inhibition control would serve as a robust neurobiological marker for evaluating both MPH and ATX effects. In summary, we explored the feasibility of introducing fNIRS-based neuropharmacological assessment of the effects of MPH/ATX administration to ADHD children, and concluded that the right IFG and MFG activation could serve as robust objective neurobiological markers to visualize the effects of MPH/ATX on ADHD children based on the following observations.

4. Study 2 individual differentiation between ADHD and healthy control children using multichannel fNIRS, emphasizing how spatial distribution and amplitude of hemodynamic response associated with go/no-go task execution can be utilized

The purpose of Study 2 was to explore the possibility of fNIRS-based single-subject diagnosis with various technical approaches. The exploration of fNIRS-based individual classification methodology has been attracting increasing research interest with extremely promising results pertaining to its use for the clinical diagnosis of psychiatric and neurodevelopmental disorders. Recently, a multi-site large-scale fNIRS study involving over 600 adult subjects suffering from bipolar disorder, depressive disorder, and schizophrenia demonstrated high classification accuracy using disorder-specified hemodynamic response patterns: sensitivity of differentiation from healthy control subjects was 76.9% for bipolar disorder, 74.6% for major depressive disorder, and 90.0% for schizophrenia [74]. Furthermore, in a different study enrolling nine boys with medicated ADHD and eight boys with autism spectrum disorder (ASD), use of a support vector machine on hemodynamic response data during a task involving viewing the subject's mother's face allowed the discrimination of the two populations with an 84% accuracy of classification [75].

In our previous session, described above, we introduced fNIRS-based monitoring of the neuropharmacological effects of ADHD medications. Furthermore, with group analyses, we successfully visualized differential neural substrates for ADHD and healthy control children for inhibitory control. The inhibition task recruited the right IFG/MFG, and activation was significantly high during the go/no-go task (Cohen's *d*: 1.009). Those results led us to postulate that right IFG/MFG activations for a go/no-go task, as observed using fNIRS, might be used as an objective neuro-functional biomarker to differentiate school-aged ADHD children and healthy controls at the individual level. Consequently, our next challenge was to explore the inhibition-related dysfunction in ADHD children at an individual level.

We explored a method for individual classification between ADHD and healthy control subjects using fNIRS, emphasizing how spatial distribution and amplitude of the hemodynamic response associated with go/no-go task execution can be utilized. To do this, we needed to identify the cut-off amplitude of cortical activation of each ROI mentioned above in order to differentiate ADHD children from healthy control children. We focused on individual oxy-Hb signal change during target (go/no-go) sessions at multichannel locations for the right MFG and IFG, where a go/no-go-task-related activation in control subjects was conspicuously large

at a single-channel location in group analyses from our previous studies [76–78]. In order to identify a robust classification parameter, we adopted the right MFG and IFG as ROIs (call optimized ROIs). Then, making the best use of multichannel analysis, we adapted well-formed formulae to identify the constituent CHs of the optimized ROIs, and assessed whether a specific logic could improve the efficacy of classification.

First, we screened for any fNIRS channels involved in the go/no-go task for control and ADHD subjects at the group level (**Figure 4**). We found significant oxy-Hb increase in three CHs in the right (R) hemisphere, including R CH 5 (mean 0.057, SD 0.077, $p < 0.05$, Bonferroni-corrected, Cohen's $d = 0.741$), R CH 6 (mean 0.046, SD 0.060, $p < 0.05$, Bonferroni-corrected, Cohen's $d = 0.755$), and R CH 10 (mean 0.068, SD 0.065, $p < 0.05$, Bonferroni-corrected, Cohen's $d = 1.046$) in control subjects. Conversely, ADHD conditions showed no significant oxy-Hb increase in the measured cortical areas. Thus, we adopted CHs 5, 6, and 10 as statistically specific ROIs to represent the channels activated for go/no-go task execution in healthy control subjects. We performed independent two-sample *t*-tests (two-tails) on these contrasts with a statistical threshold of $p < 0.05$.

Second, we assessed the group difference in oxy-Hb signals among the ROIs (**Figure 3**). The comparison between ADHD and healthy control subjects revealed significant activation of oxy-Hb signal in the right CHs 6 and 10 in the control subjects than in ADHD subjects at the group level (independent two-sample *t*-test; R CH 6, $p < 0.05$ Bonferroni-corrected, Cohen's $d = 0.964$; R CH 10, $p < 0.05$ Bonferroni-corrected, Cohen's $d = 0.699$). The right CHs 6 and 10 were located in the border region between the right MFG and IFG (R CH 6, MNI coordinates x, y, z (SD): 59, 28, 19 (25), MFG 18%, IFG 52%; R CH 10, MNI coordinates x, y, z (SD): 48, 37, 34 (27), MFG 63%, IFG 31%) in reference to a macroanatomical brain atlas [68].

We applied CHs 6 and 10 as statistically robust ROIs to represent the most significant activation in healthy control compared with ADHD subjects during go/no-go task execution. In order to

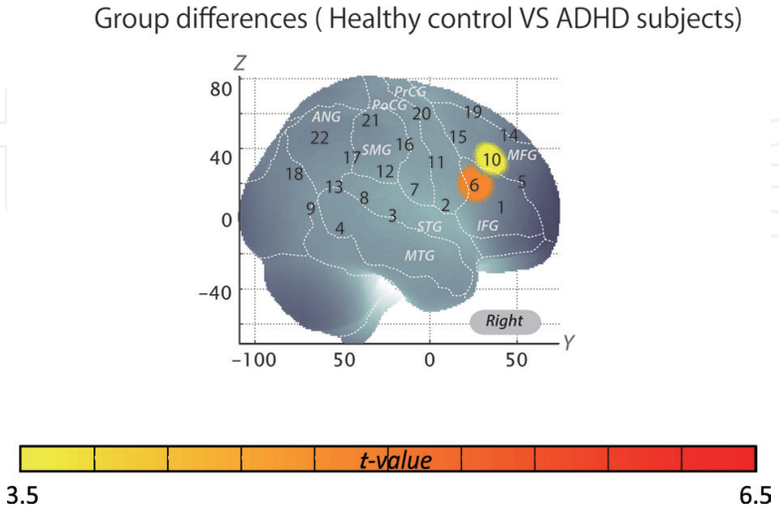

Figure 3. Cortical activation patterns for group-level comparison between the ADHD and healthy control groups during a go/no-go task. t-Maps of oxy-Hb signals are displayed, with significant *t*-values (paired *t*-test, Bonferroni-corrected) shown according to the color bar.

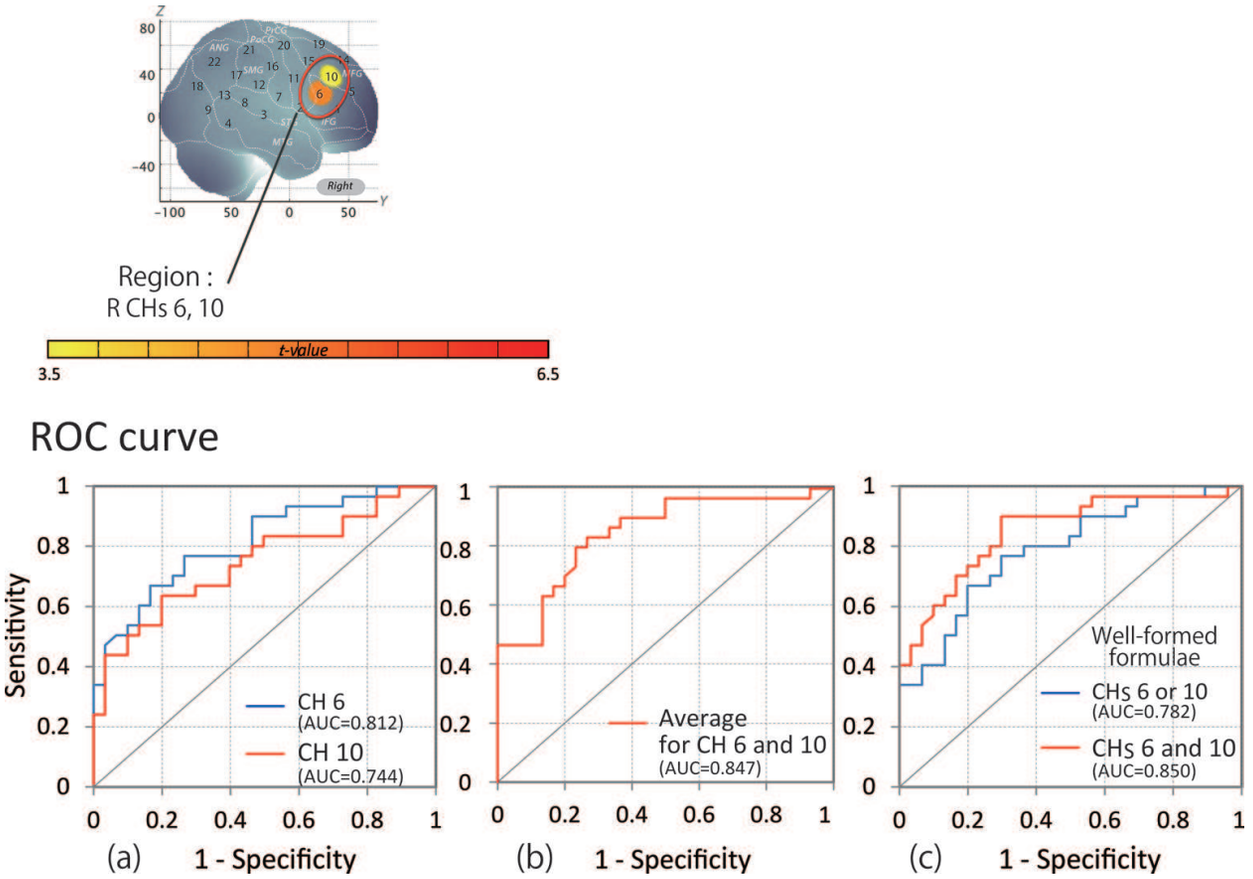

Figure 4. In order to predict ADHD diagnosis using channel-wised hemodynamic changes, we applied CHs 6 and 10 as statistically robust ROIs to represent the most significant activation in healthy control compared with ADHD subjects during go/no-go task execution. We explored setting a cut-off value for individual fNIRS-based oxy-Hb signal patterns: (a) CHs 6 and 10, respectively, (b) average oxy-Hb signal contrasts for the right CHs 6 and 10, (c) optimized values using well-formed formulae. For each cut-off value, sensitivity and 1-specificity to create a receiver operating characteristic (ROC) were plotted. Subsequently, the area under the resultant ROC curve (AUC) was calculated. Finally, the best cut-off value was identified as that with the highest sensitivity and specificity, which is the point nearest to the top left corner of the curve.

classify ADHD and healthy control children with higher accuracy, we explored setting a cut-off value for individual fNIRS-based oxy-Hb signal patterns. We set the initial cut-off value for the oxy-Hb signal at 0 mM·mm. From this start point, the cut-off value was incremented or diminished until specificity or sensitivity reached 0 or 1. For each cut-off value, we plotted sensitivity and 1-specificity to create a receiver operating characteristic (ROC). In addition, we calculated the area under the resultant ROC curve (AUC). Then the best cut-off value was identified as that with the highest sensitivity and specificity, which is the point nearest to the top left corner of the curve (**Figure 4**). In this and in the previous study, the PASW Statistics (version 18 for Windows) (SPSS Inc., Chicago, USA) software package was used for statistical analyses.

First, we examined each channel (CH 6 and 10) component. For CH 6, the AUC value was 81.20%. At the optimal cut-off value of 0.0000 mM·mm, differentiation between ADHD and healthy control subjects was achieved with a sensitivity of 66.7% and a specificity of

83.3% (**Figure 4(a)**). For CH 10, the AUC value was 74.4%. At the optimal cut-off value of 0.0320 mM·mm, differentiation between ADHD and healthy control subjects was achieved with a sensitivity of 63.3% and a specificity of 80.0% (**Figure 4(a)**). Second, the averages of the integral values for CHs 6 and 10 for 30 individual ADHD and healthy control subjects were calculated (**Figure 4(b)**). The resulting AUC value was 84.7%. At the optimal cut-off value of 0.0374 mM·mm, differentiation between ADHD and healthy control subjects was achieved with a sensitivity of 83.3% and a specificity of 73.3% (**Figure 4(a)**).

Third, for further optimization, we adapted well-formed formulae for CHs 6 and 10 in the most optimized ROI. With "AND" logic, a subject was classified as normal (not ADHD), when the subject's oxy-Hb signals for CHs 6 "AND" 10 were above a given threshold. When "OR" logic was applied, a subject was classified as normal (not ADHD), when the subject's oxy-Hb signal for CH 6 "OR" 10 was above a given threshold. For each classification using well-formed formulae, ROC analysis was performed as described above. We adapted well-formed formulae for CHs 6 and 10 to better classify ADHD and healthy control subjects. When "OR" logic was adopted, the area under the AUC was 78.2%. At the optimal cut-off value of 0.0650 mM·mm, differentiation between ADHD and healthy control subjects was achieved with a sensitivity of 76.7% and a specificity of 70.0% (**Figure 4**). Finally, when "AND" logic was adopted, the AUC value was 85.0%, which was the highest percentage among all classifications. At the optimal cut-off value of 0.0111 mM·mm, differentiation between ADHD and healthy control subjects was achieved with a sensitivity of 90.0% and a specificity of 70.0% (**Figure 4**).

5. Study 2: Discussion

Optimized ROIs in the right IFG and MFG to differentiate ADHD children from healthy control children were successfully identified through individual assessment of channel-wise oxy-Hb signal changes using fNIRS; adaptation of well-formed formulae to two CHs to form optimized ROIs achieved 90% sensitivity for diagnostic predictions at the individual level. Thus, we suggest the high possibility that this novel fNIRS-based measurement may serve as an efficient diagnostic method to enable differentiation between ADHD and healthy children at an individual level. Previous neuroimaging studies have reported on methods for diagnostic classification of ADHD and healthy control subjects at the individual level that adopt multifactorial methods (e.g., neuroanatomical pattern classification) to structural MRI data [43, 79] and to fMRI data [37, 80–84]. However, our protocol requires only a single variable (the simple "integral value" of fNIRS signals for only two ROIs) and produces high classification rates (sensitivity: 90%). Our classification rates were equivalent to those reported for previous MRI and fMRI studies using multivariate statistical methods, which ranged from 67 to 93% for ADHD groups compared with healthy control children.

Recently, a considerable number of studies have introduced neural correlates for go/no-go tasks, including the right IFG and MFG [60]. Furthermore, a recent activation likelihood estimation (ALE) meta-analysis of go/no-go tasks [85] revealed a mainly right-lateralized network associated with response inhibition, including the right MFG and IFG (BA46/44) [70].

The right IFG and MFG have been implicated in processes of response selection, stimulus recognition, and maintenance and manipulation of stimulus-response associations, including selecting not to respond, all of which are critical in the performance of go/no-go tasks.

From a genetic perspective, the catechol-O-methyltransferase (COMT) gene [86], the dopamine active transporter 1 gene (DAT1, also known as SLC6A3), and the dopamine receptor D4 (DRD4) gene [39] are deeply associated with the pathophysiology of ADHD. These genes are thought to be involved in the monoamine system, and their dysfunction in the prefrontal cortex, including the IFG and MFG, is considered to be the core pathomechanism of ADHD.

6. Limitations Study 1 & 2

As discussed above, the current study has demonstrated that our fNIRS-based experimental method of using inhibition-elicited cerebral functional to differentiate between ADHD and healthy control children allows the observation of a distinct biological marker in clinical situations. However, before establishing its utility in clinical practice, several issues need to be addressed.

First, the scope of the current study does not necessarily extend to screening for ADHD with comorbidity. Therefore, our next step is to explore the disorder-specificity of fNIRS-based individual classification relative to other developmental and psychiatric disorders, such as autism spectrum disorder, oppositional defiant disorder, conduct disorder, depression, and anxiety.

Second, although most ADHD subjects had temporally stopped medication (MPH or ATX) for more than 48 hours before fNIRS examination, the condition of the ADHD subjects in this study may not precisely reflect immune brain activation. Several other neuroimaging studies examining medication-naïve ADHD patients have been reported in a recent meta-analysis [87]. Brain function can be changed with long-term MPH and ATX administration; the recent meta-analysis of human studies using fMRI suggested that long-term MPH treatment is associated with more normal activation in the right DLPFC. Therefore, we need to explore medication-naïve ADHD patients as our next step.

Author details

Yukifumi Monden[1,2,3]*, Masako Nagashima[1], Haruka Dan[2], Takahiro Ikeda[1], Yasushi Kyutoku[2], Takanori Yamagata[1] and Ippeita Dan[2]

*Address all correspondence to: mon4441977319@jichi.ac.jp

1 Department of Pediatrics, Jichi Medical University, Tochigi, Japan

2 Applied Cognitive Neuroscience Laboratory, Chuo University, Tokyo, Japan

3 Department of Pediatrics, International University of Health and Welfare, Tochigi, Japan

References

[1] Obrig H, Villringer A. Beyond the visible-imaging the human brain with light. Journal of Cerebral Blood Flow & Metabolism. 2003;**23**:1-18. DOI: 10.1097/01.WCB.0000043472.45775.29

[2] Strangman G, Boas DA, Sutton JP. Non-invasive neuroimaging using near-infrared light. Biological Psychiatry. 2002;**52**:679-693

[3] Ferrari M, Quaresima V. A brief review on the history of human functional near-infrared spectroscopy (fNIRS) development and fields of application. NeuroImage. 2012;**63**:921-935. DOI: 10.1016/j.neuroimage.2012.03.049

[4] Minagawa-Kawai Y, Mori K, Hebden JC, et al. Optical imaging of infants' neurocognitive development: Recent advances and perspectives. Developmental Neurobiology. 2008;**68**:712-728. DOI: 10.1002/dneu.20618

[5] Lloyd-Fox S, Blasi SA, Elwell CE. Illuminating the developing brain: The past, present and future of functional near infrared spectroscopy. Neuroscience and Biobehavioral Reviews. 2010;**34**:269-284. DOI: 10.1016/j.neubiorev.2009.07.008

[6] Okamoto M, Dan H, Shimizu K, et al. Multimodal assessment of cortical activation during apple peeling by NIRS and fMRI. NeuroImage. 2004;**21**:1275-1288. DOI: 10.1016/j.neuroimage.2003.12.003

[7] Hock C, Villringer K, Muller-Sphan F, et al. Decrease in parietal cerebral hemoglobin oxygenation during performance of a verbal fluency task in patients with Alzheimer's disease monitored by means of near-infrared spectroscopy (NIRS) – correlation with simultaneous rCBF-PET measurements. Brain Research. 1997;**755**:293-303

[8] Suto T, Fukuda M, Ito M, et al. Multichannel near-infrared spectroscopy in depression and schizophrenia: Cognitive brain activation study. Biological Psychiatry. 2004;**55**:501-511. DOI: 10.1016/j.biopsych.2003.09.008

[9] Herrmann MJ, Plichta MM, Ehlis AC, et al. Optical topography during a Go-NoGo task assessed with multi-channel near-infrared spectroscopy. Behavioural Brain Research. 2005;**160**:135-140. DOI: 10.1016/j.bbr.2004.11.032

[10] Okamoto M, Matsunami M, Dan H, et al. Prefrontal activity during taste encoding: An fNIRS study. NeuroImage. 2006;**31**:796-806. DOI: 10.1016/j.neuroimage.2005.12.021

[11] Moriai-Izawa A. Multichannel fNIRS assessment of overt and covert confrontation naming. Brain and Language. 2012;**121**:185-193

[12] Miyai I, Dan H, Dan I, et al. Cortical mapping of gait in humans: A near-infrared spectroscopic topography study. NeuroImage. 2001;**14**:1186-1192. DOI: 10.1016/j.bandl.2012.02.001

[13] Murata Y, Sakatani K, Katayama Y, et al. Increase in focal concentration of deoxyhaemoglobin during neuronal activity in cerebral ischaemic patients. Journal of Neurology, Neurosurgery, and Psychiatry. 2002;**73**:182-184

[14] Watanabe E, Maki A, Kawaguchi F, et al. Noninvasive cerebral blood volume measurement during seizures using multichannel near infrared spectroscopic topography. Journal of Biomedical Optics. 2000;**5**:287-290. DOI: 10.1117/1.429998

[15] Watanabe E, Nagahori Y, Mayanagi Y, Focus Y. Diagnosis of epilepsy using near-infrared spectroscopy. Epilepsia. 2002;**43**:50-55

[16] Nguyen DK, Tremblay J, Pouliot P, et al. Noninvasive continuous functional near-infrared spectroscopy combined with electroencephalography recording of frontal lobe seizures. Epilepsia. 2012;**54**:331-340. DOI: 10.1111/epi.12011

[17] Hahn T, Marquand AF, Plichta MM, et al. A novel approach to probabilistic biomarker-based classification using functional near-infrared spectroscopy. Human Brain Mapping. 2012;**34**:1102-1114. DOI: 10.1002/hbm.21497

[18] Weber P, Lutschg J, Fahnenstich H, Cerebral H. Hemodynamic changes in response to an executive function task in children with attention-deficit hyperactivity disorder measured by near-infrared spectroscopy. Journal of Developmental and Behavioral Pediatrics. 2005;**26**:105-111

[19] Ehlis AC, Bähne CG, Jacob CP, et al. Reduced lateral prefrontal activation in adult patients with attention-deficit/hyperactivity disorder (ADHD) during a working memory task: A functional near-infrared spectroscopy (fNIRS) study. Journal of Psychiatric Research. 2008;**42**:1060-1067. DOI: 10.1016/j.jpsychires.2007.11.011

[20] Schecklmann M, Ehlis AC, Plichta MM, et al. Diminished prefrontal oxygenation with normal and above-average verbal fluency performance in adult ADHD. Journal of Psychiatric Research. 2008;**43**:98-106. DOI: 10.1016/j.jpsychires.2008.02.005

[21] Schecklmann M, Romanos M, Bretscher F, et al. Prefrontal oxygenation during working memory in ADHD. Journal of Psychiatric Research. 2010;**44**:621-628. DOI: 10.1016/j.jpsychires.2009.11.018

[22] Negoro H, Sawada M, Iida J, et al. Prefrontal dysfunction in attention-deficit/hyperactivity disorder as measured by near-infrared spectroscopy. Child Psychiatry and Human Development. 2010;**41**:193-203. DOI: 10.1007/s10578-009-0160-y

[23] Inoue Y, Sakihara K, Gunji A, et al. Reduced prefrontal hemodynamic response in children with ADHD during the go/no-go task: A NIRS study. Neuroreport. 2011;**23**:55-60. DOI: 10.1097/WNR.0b013e32834e664c.

[24] Dittmann RW, Wehmeier PM, Schacht A, et al. Atomoxetine treatment and ADHD-related difficulties as assessed by adolescent patients, their parents and physicians. Child Adolesc Psychiatry Ment Health. 2009;**3**(1):21. DOI: 10.1186/1753-2000-3-21

[25] Craig F, Margari F, Legrottaglie AR, et al. A review of executive function deficits in autism spectrum disorder and attention-deficit/hyperactivity disorder. Neuropsychiatric Disease and Treatment. 2016;**12**:1191-1202. DOI: 10.2147/NDT.S104620.eCollection 2016

[26] Drechsler R, Brandeis D, Földényi M, et al. The course of neuropsychological functions in children with attention deficit hyperactivity disorder from late childhood to early adolescence. Journal of Child Psychology and Psychiatry. 2005;**46**:824-836

[27] Lahey BB, Applegate B, Waldman ID, et al. The structure of child and adolescent psychopathology: Generating new hypotheses. Journal of Abnormal Psychology. 2004;**113**:358-385

[28] Safren SA, Sprich S, Mimiaga MJ, et al. Cognitive behavioral therapy vs relaxation with educational support for medication-treated adults with ADHD and persistent symptoms: A randomized controlled trial. Journal of the American Medical Association. 2010;**304**:875-880. DOI: 10.1001/jama.2010.1192

[29] Power TJ, Shapiro ES, DuPaul GJ. Preparing psychologists to link systems of care in managing and preventing children's health problems. Journal of Pediatric Psychology. 2003;**28**:147-155

[30] Bruchmuller K, Margraf J, Schneider S. Is ADHD diagnosed in accord with diagnostic criteria? Overdiagnosis and influence of client gender on diagnosis. Journal of Consulting and Clinical Psychology. 2012;**80**:128-138. DOI: 10.1037/a0026582

[31] Batstra L, Hadders-Algra M, Nieweg E, et al. Childhood emotional and behavioral problems: Reducing overdiagnosis without risking undertreatment. Developmental Medicine and Child Neurology. 2012;**54**:492-494. DOI: 10.1111/j.1469-8749.2011.04176.x

[32] Wolraich M, Brown L, Brown RT, et al. ADHD: Clinical practice guideline for the diagnosis, evaluation, and treatment of attention-deficit/hyperactivity disorder in children and adolescents. Pediatrics. 2011;**128**:1007-1022. DOI: 10.1542/peds.2011-2654

[33] Pliszka S. Practice parameter for the assessment and treatment of children and adolescents with attention-deficit/hyperactivity disorder. Journal of the American Academy of Child and Adolescent Psychiatry. 2007;**46**:894-921

[34] Taylor E, Döpfner M, Sergeant J, et al. European clinical guidelines for hyperkinetic disorder – first upgrade. European Child & Adolescent Psychiatry. 2004;**13**:17-30

[35] Hodgkins P, Shaw M, Coghill D, et al. Amfetamine and methylphenidate medications for attention-deficit/hyperactivity disorder: Complementary treatment options. European Child & Adolescent Psychiatry. 2012;**21**(9):477-492. DOI: 10.1007/s00787-012-0286-5

[36] Spencer TJ. ADHD treatment across the life cycle. The Journal of Clinical Psychiatry. 2004;**65**:22-26

[37] Zhu CZ, Zang YF, Cao QJ, et al. Fisher discriminative analysis of resting-state brain function for attention-deficit/hyperactivity disorder. NeuroImage. 2008;**40**:110-120. DOI: 10.1016/j.neuroimage.2007.11.029

[38] Wehmeier PM, Schacht A, Barkley RA. Social and emotional impairment in children and adolescents with ADHD and the impact on quality of life. The Journal of Adolescent Health. 2010;**46**:209-217. DOI: 10.1016/j.jadohealth.2009.09.009

[39] Leitner Y. The co-occurrence of autism and attention deficit hyperactivity disorder in children – What do we know? Frontiers in Human Neuroscience. 2014;**8**:268. DOI: 10.3389/fnhum.2014.00268. eCollection 2014

[40] Barkley RA. Behavioral inhibition, sustained attention, and executive functions: Constructing a unifying theory of ADHD. Psychological Bulletin. 1997;**121**:65-94

[41] Dillo W, Göke A, Prox-Vagedes V, et al. Neuronal correlates of ADHD in adults with evidence for compensation strategies – A functional MRI study with a go/no-go paradigm. German Medical Science. 2010;**8**:9. DOI: 10.3205/000098

[42] Bush G, Frazier JA, Rauch SL, et al. Anterior cingulate cortex dysfunction in attention-deficit/hyperactivity disorder revealed by fMRI and the counting Stroop. Biological Psychiatry. 1999;**45**:1542-1552

[43] Durston S, Tottenham NT, Thomas KM, et al. Differential patterns of striatal activation in young children with and without ADHD. Biological Psychiatry. 2003;**53**:871-878

[44] Vaidya CJ, Austin G, Kirkorian G, et al. Selective effects of methylphenidate in attention deficit hyperactivity disorder: A functional magnetic resonance study. Proceedings of the National Academy of Sciences of the United States of America. 1998;**95**:14494-14499

[45] Rubia K, Overmeyer S, Taylor E, et al. Hypofrontality in attention deficit hyperactivity disorder during higher-order motor control: A study with functional MRI. The American Journal of Psychiatry. 1999;**156**(6):891

[46] Levin HS et al. Developmental changes in performance on tests of purported frontal lobe functioning. Developmental Neuropsychology. 1991;**7**:377-395

[47] Comalli PE, Wapner S Jr, Werner H. Interference effects of Stroop color-word test in childhood, adulthood, and aging. The Journal of Genetic Psychology. 1962;**100**:47-53

[48] Williams BR, Ponesse JS, Schachar RJ, et al. Development of inhibitory control across the life span. Developmental Psychology. 1999;**35**(1):205-213

[49] Durston S, Hulshoff Pol HE, Schnack HG, et al. Magnetic resonance imaging of boys with attention-deficit/hyperactivity disorder and their unaffected siblings. Journal of the American Academy of Child and Adolescent Psychiatry. 2004;**43**:332-340

[50] Monden Y, Dan H, Nagashima M, et al. Clinically-oriented monitoring of acute effects of methylphenidate on cerebral hemodynamics in ADHD children using fNIRS. Clinical Neurophysiology. 2011;**123**:1147-1157. DOI: 10.1016/j.clinph.2011.10.006.

[51] Cope M, Delpy DT, Reynolds EO, et al. Methods of quantitating cerebral near infrared spectroscopy data. Adv Exp Med Biol. 1988;**222**:183-189

[52] Maki A, Yamashita Y, Ito Y, Watanabe E, et al. Spatial and temporal analysis of human motor activity using noninvasive NIR topography. Medical Physics. 1995;**22**:1997-2005

[53] Strangman G, Culver JP, Thompson JH, et al. A quantitative comparison of simultaneous BOLD fMRI and NIRS recordings during functional brain activation. NeuroImage. 2002;**17**:719-731

[54] Hoshi Y, Kobayashi N, Tamura M. Interpretation of near-infrared spectroscopy signals: A study with a newly developed perfused rat brain model. Journal of Applied Physiology. 2001;**90**:1657-1662

[55] Hoshi Y. Functional near-infrared optical imaging: Utility and limitations in human brain mapping. Psychophysiology. 2003;**40**:511-520

[56] Plichta M, Herrmann MJ, Baehne CG, et al. Event-related functional near-infrared spectroscopy (fNIRS): Are the measurements reliable? NeuroImage. 2006;**31**:116-124

[57] Garavan H, Ross TJ, Stein EA. Right hemispheric dominance of inhibitory control: An event-related functional MRI study. Proceedings of the National Academy of Sciences of the United States of America. 1999;**96**:8301-8306

[58] Herrmann M, Ehlis AC, Fallgatter A. Bilaterally reduced frontal activation during a verbal fluency task in depressed patients as measured by near-infrared spectroscopy. The Journal of Neuropsychiatry and Clinical Neurosciences. 2004;**16**:170-175

[59] Liddle PF, Kiehl KA, Smith AM. Event-related fMRI study of response inhibition. Human Brain Mapping. 2001;**12**:100-109

[60] Rubia K, Smith AB, Brammer MJ, et al. Right inferior prefrontal cortex mediates response inhibition while mesial prefrontal cortex is responsible for error detection. NeuroImage. 2003;**20**:351-358

[61] Tsuzuki D, Dan I. Spatial registration for functional near-infrared spectroscopy: From channel position on the scalp to cortical location in individual and group analyses. NeuroImage. 2014;**85**:92-103. DOI: 10.1016/j.neuroimage.2013.07.025

[62] Tsuzuki D, Jurcak V, Singh AK, et al. Virtual spatial registration of stand-alone fNIRS data to MNI space. NeuroImage. 2007;**34**:1506-1518

[63] Brett M, Johnsrude LS, Owen AM. The problem of functional localization in the human brain. Nature Reviews Neuroscience. 2002;**3**:243-249

[64] Okamoto M, Dan H, Sakamoto K, et al. Three-dimensional probabilistic anatomical cranio-cerebral correlation via the international 10-20 system oriented for transcranial functional brain mapping. NeuroImage. 2004;**21**:99-111

[65] Okamoto M, Dan I. Automated cortical projection of head-surface locations for transcranial functional brain mapping. NeuroImage. 2005;**26**(1):18-28

[66] Singh AK, Dan I. Exploring the false discovery rate in multichannel NIRS. NeuroImage. 2006;**33**:542-549

[67] Shattuck DW, Mirza M, Adisetiyo V, et al. Construction of a 3D probabilistic atlas of human cortical structures. NeuroImage. 2008;**39**:1064-1080

[68] Rorden C, Brett M. Stereotaxic display of brain lesions. Behavioural Neurology. 2000;**12**:191-200

[69] Katagiri A, Dan I, Tuzuki D, et al. Mapping of optical pathlength of human adult head at multi-wavelengths in near infrared spectroscopy. Adv Exp Med Biol. pp. 205-212. DOI: 10.1007/978-1-4419-1241-1_29, 10.1007/978-1-4419-1241-1_29

[70] Simmonds DJ, Pekar JJ, Mostofsky SH. Meta-analysis of go/no-go tasks demonstrating that fMRI activation associated with response inhibition is task-dependent. Neuropsychologia. 2008;**46**:224-232

[71] Araki A, Ikegami M, Okayama A, et al. Improved prefrontal activity in AD/HD children treated with atomoxetine: A NIRS study. Brain & Development. 2015;**37**:76-87. DOI: 10.1016/j.braindev.2014.03.011

[72] Ishii-Takahashi A, Takizawa R, Nishimura Y, et al. Neuroimaging-aided prediction of the effect of methylphenidate in children with attention-deficit hyperactivity disorder: A randomized controlled trial. Neuropsychopharmacology. 2015;**40**:2676-2685. DOI: 10.1038/npp.2015.154

[73] Aron AR, Poldrack RA. The cognitive neuroscience of response inhibition: Relevance for genetic research in attention-deficit/hyperactivity disorder. Biological Psychiatry. 2005;**57**:1285-1292

[74] Takizawa R, Fukuda M, Kawasaki S, et al. Neuroimaging-aided differential diagnosis of the depressive state. NeuroImage. 2014;**85**:498-507. DOI: 10.1016/j.neuroimage.2013.05.126

[75] Ichikawa H, Kitazono J, Nagata K, et al. Novel method to classify hemodynamic response obtained using multi-channel fNIRS measurements into two groups: Exploring the combinations of channels. Frontiers in Human Neuroscience. 2014;**8**:480. DOI: 10.3389/fnhum.2014.00480.eCollection 2014

[76] Monden Y, Dan H, Nagashima M, et al. Right prefrontal activation as a neuro-functional biomarker for monitoring acute effects of methylphenidate in ADHD children: An fNIRS study. NeuroImage: Clinical. 2012;**1**:131-140. DOI: 10.1016/j.nicl.2012.10.001.eCollection 2012

[77] Monden Y, Dan H, Nagashima M, et al. Clinically-oriented monitoring of acute effects of methylphenidate on cerebral hemodynamics in ADHD children using fNIRS. Clinical Neurophysiology. 2012;**123**:1147-1157. DOI: 10.1016/j.clinph.2011.10.006 Epub Nov 15, 2011

[78] Nagashima M, Monden Y, Dan I, et al. Acute neuropharmacological effects of atomoxetine on inhibitory control in ADHD children: A fNIRS study. NeuroImage: Clinical. 2014;**6**:192-201. DOI: 10.1016/j.nicl.2014.09.001.eCollection 2014

[79] Johnston BA, Mwangi B, Matthews K, et al. Brainstem abnormalities in attention deficit hyperactivity disorder support high accuracy individual diagnostic classification. Human Brain Mapping. 2014;**35**:5179-5189. DOI: 10.1002/hbm.22542 Epub May 13, 2014

[80] Solmaz B. ADHD classification using bag of words approach on network features. In: SPIE Medical Imaging. International Society for Optics and Photonics; 2012

[81] Colby JB. Insights into multimodal imaging classification of ADHD. Frontiers in Systems Neuroscience. 2012;**16**;6:59. DOI: 10.3389/fnsys.2012.00059. eCollection 2012

[82] Dai D, Rudie JD, Brown JA, et al. Classification of ADHD children through multimodal magnetic resonance imaging. Frontiers in Systems Neuroscience. 2012;**6**(3):63. DOI: 10.3389/fnsys.2012.00063. eCollection 2012

[83] Hoekzema E, Carmona S, Ramos-Quiroga JA, et al. An independent components and functional connectivity analysis of resting state fMRI data points to neural network dysregulation in adult ADHD. Hum Brain Mapp. Apr; 2014;**35**:1261-1272. DOI: 10.1002/hbm.22250. Epub 2013 Feb 18

[84] Hart H. Pattern classification of response inhibition in ADHD: Toward the development of neurobiological markers for ADHD. Human Brain Mapping. 2014;**35**:3083-3094

[85] Buchsbaum BR, Greer S, Chang WL, et al. Meta-analysis of neuroimaging studies of the Wisconsin card-sorting task and component processes. Human Brain Mapping. 2005;**25**:35-45

[86] Taurines R, Schwenck C, Westerwald E, et al. ADHD and autism: Differential diagnosis or overlapping traits? A selective review. Attention Deficit and Hyperactivity Disorders. 2012;**4**:115-139. DOI: 10.1007/s12402-012-0086-2

[87] Hart H, Radua J, Mataix-Cols D, Rubia K. Meta-analysis of fMRI studies of timing in attention-deficit hyperactivity disorder (ADHD). Neuroscience and Biobehavioral Reviews. 2012;**36**:2248-2256

IntechOpen